ACS APPLIED ELECTRONIC MATERIALS

pubs.acs.org/acsaelm Article

An Ionic Hydrogel-Based Antifreezing Triboelectric Nanogenerator

Binbin Ying, Runze Zuo, Yilun Wan, and Xinyu Liu*

Cite This: ACS Appl. Electron. Mater. 2022, 4, 1930−1938 Read Online

ACCESS | Metrics & More | Article Recommendations | Supporting Information

ABSTRACT: The rapid development of stretchable electronics and soft robotics requires a sustainable power source that can match their mechanical stretchability in various working environments. Ionic hydrogel-based soft triboelectric nanogenerators (TENGs) show great promise for those application scenarios. However, ionic hydrogel-based TENGs suffer from the freezing issue under subzero temperatures. In this study, a low-cost, highly stretchable, and antifreezing ionic triboelectric nanogenerator (iTENG) is designed to involve a dielectric elastomer and a freeze-tolerant ionic hydrogel as the electrification layer and the electrode, respectively. The iTENG design achieves a unique combination of merits such as robust hydrogel−elastomer bonding, high stretchability (300%), and excellent tolerance of extremely low temperature (down to −53 °C). Because of the reliable interfacial bonding, the iTENG shows a good mechanical durability under different stretching conditions. The iTENG can harvest mechanical energies from various human motions and can also serve as a self-powered wearable sensor in both regular and extremely cold environments. The stretchable iTENG overcomes the strain-induced performance degradation of existing stretchable materials with percolated conductive fillers and the water freezing-induced degradation of conductive ionic hydrogels, providing a feasible design of stretchable and sustainable power sources for stretchable electronics and soft robotics operating in harsh environments.

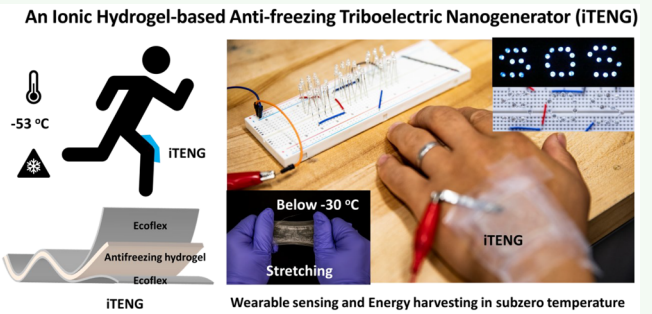

KEYWORDS: *stretchable electronics, antifreezing ionic hydrogel, triboelectric nanogenerator, energy harvesting, soft robotics*

INTRODUCTION

The rapid growth of wearable electronics and soft robotics relies on power sources that are mechanically flexible, stretchable, and even biocompatible. So far, flexible energy storage devices (e.g., supercapacitors[1−3] and batteries[4]) have been developed to reduce the mechanical constraint on the bodies of humans and soft robots when being worn. However, most of these energy sources lack the self-charging capability. On the other hand, flexible energy harvesting devices such as solar cells and nanogenerators have been developed in the past decade to realize sustainable power sources for flexible systems.[5−8] For example, triboelectric nanogenerators (TENGs) can convert mechanical energies into electricity based on the coupling effect of contact electrification and electrostatic induction. Recently, TENGs have attracted tremendous attention as promising mechanical energy harvesting devices due to their advantages such as high degree of freedom for material selection, high voltage output, simple structure, easy fabrication, good environmental friendliness, and low cost.[9−14]

To date, conductive materials such as carbon nanotubes, graphene, carbon paste, and silver nanowires[15−18] have been utilized for the construction of stretchable TENGs. Nevertheless, the sheet resistance of existing TENGs increases remarkedly at large strains (e.g., >100%) because the percolated networks of those conductive fillers in the stretchable substrates are greatly affected by the material deformation;[19] this limits their suitability for application scenarios involving large strains. Alternatively, TENGs with ultrahigh stretchability have been developed by using ionic liquid-based gels (ionogels).[20−23] Those as-fabricated devices possess practically useful features such as ambient stability and antifreezing capability due to the intrinsically nonvolatile characteristics of the ionic liquids. Therefore, ionogel-based TENGs can realize mechanical energy harvesting over a wide temperature range.[24] However, the broad application of ionogels to the designs of TENGs and other stretchable electronics was still limited by their high cost, complex synthesis procedure, relatively low conductivity, low mechanical toughness, and the toxicity of ionic liquids.

Hydrated and ionic materials such as deformable and tough ionic hydrogels have been regarded as one of the most ideal stretchable materials for electronic applications[25] because of

Received: January 24, 2022
Accepted: March 8, 2022
Published: March 24, 2022

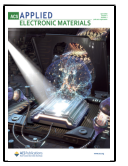

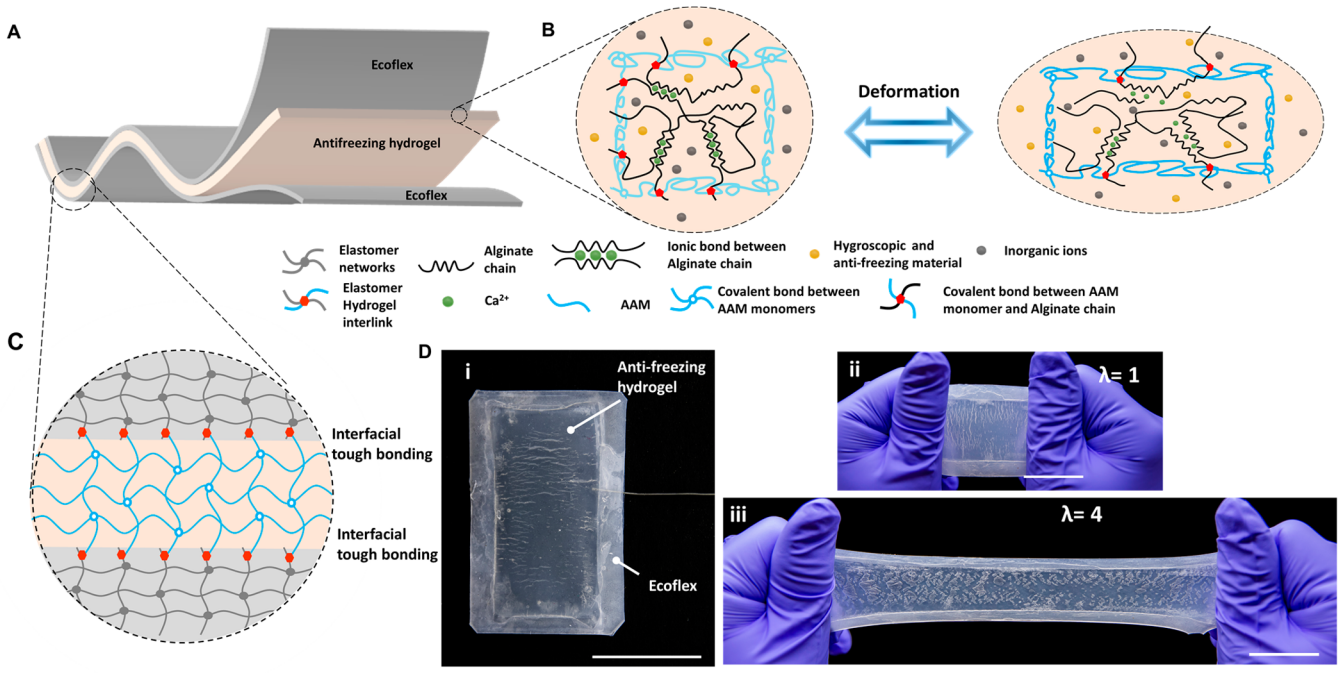

Figure 1. Design of antifreezing and stretchable iTENG with robust interfacial bonding. (A) Scheme of the iTENG with a sandwich architecture. (B) Schematic illustration of the antifreezing hydrogel under deformation. The antifreezing hydrogel is made from a tough double-network (DN) hydrogel matrix containing both ionically (the black alginate network) and covalently (the light blue PAAm network) cross-linked polymers. The DN hydrogel is laden with hygroscopic and antifreezing reagents (yellow dots) and inorganic ions (gray dots). (C) Schematic illustration of the tough interfacial bonding between the elastomer layer (Ecoflex) and antifreezing hydrogel due to the covalently anchored hydrogel polymer network on the elastomer surface. (D-i) An iTENG with a metal wire connected to the conductive hydrogel layer. (D-ii) An iTENG at its initial length (λ = 1). (D-iii) The iTENG stretched to 4 times its initial length (λ = 4). Scale bar: 3 cm.

their excellent biocompatibility,[26−33] high stretchability,[34] high electrical conductivity,[35] and tunable mechanical properties (e.g., toughness, stretchability, and elasticity).[36,37] Thus, ionic hydrogels have been applied to developing a variety of stretchable sensors and electronics, including pressure sensors,[38−42] strain sensors,[43] touchpads,[43,44] robotic skins,[45] and TENGs.[35] Because ionic hydrogels are solid-like, soft, highly stretchable, transparent, and biocompatible, ionic hydrogel-based TENGs show great potential as the power source for wearable electronics and soft robotics. Recently, there have been significant efforts on endowing the hydrogel-based TENGs with more practical features such as self-healing,[46,47] anticontamination,[48] and enhanced mechanical reliability (e.g., through strengthening the bonding between the conductive hydrogel and electrification elastomer).[49] However, existing hydrogel-based TENGs still suffer from the freezing issue under subzero temperatures. Regular ionic hydrogel devices cannot maintain their mechanical deformability and electrical conductivity under extremely cold conditions.

To address this challenge, this article reports a new design of an ionic hydrogel-based, antifreezing, and highly stretchable triboelectric nanogenerator (iTENG). The iTENG involves a dielectric elastomer and a freeze-tolerant ionic hydrogel as the electrification layer and the electrode, respectively, and is capable of biomechanical energy harvesting and self-powered mechanical sensing. The iTENG design achieves a unique combination of merits such as robust hydrogel−elastomer bonding, high stretchability (300%), and excellent tolerance of extremely low temperature (down to −53 °C). The soft skin-like nanogenerator can generate an open-circuit voltage up to 380 V and an instantaneous surface power density of 5.7 mW m^{-2} with good durability. The iTENG can harvest mechanical energy from various human motions and also serve as a self-powered wearable sensor in both regular and extremely cold environments. This work provides a feasible design of stretchable and sustainable power sources for stretchable electronics and soft robotics working in the harsh environments.

RESULTS AND DISCUSSION

Design of the iTENG. The iTENG has a sandwich architecture including an antifreezing ionic hydrogel layer sealed between two elastomer (Ecoflex) films (Figure 1A), and a metal belt or wire was attached to the ionic hydrogel for electrical connection. The thicknesses of antifreezing hydrogel and Ecoflex films are approximately 1.6 mm and 150 μm, respectively. The final device could be made into any two-dimensional shape. The antifreezing hydrogel was made of a tough double-network (DN) hydrogel matrix containing hygroscopic/cryoprotective substances and inorganic ions. The DN hydrogel matrix could be synthesized from a wide range of material combinations, ranging from poly(2-acrylamido-2-methylpropanesulfonic acid)−poly(acrylamide) (PAMPS−PAAm), to poly(ethylene glycol)−poly(acrylic acid) (PEG−PAA), to carrageenan−epoxy−amines, to polysaccharides−epoxy−amines, to agarose−PAAm, and to alginate (Alg)−PAAm. Specifically, hybrid cross-linked Alg−PAAm double networks were selected here because of their excellent and tunable mechanical properties (e.g., toughness and Young's modulus)[50] and good biocompatibility.[51] Cryoprotectants have been widely applied to prevent various

https://doi.org/10.1021/acsaelm.2c00118
ACS Appl. Electron. Mater. 2022, 4, 1930−1938

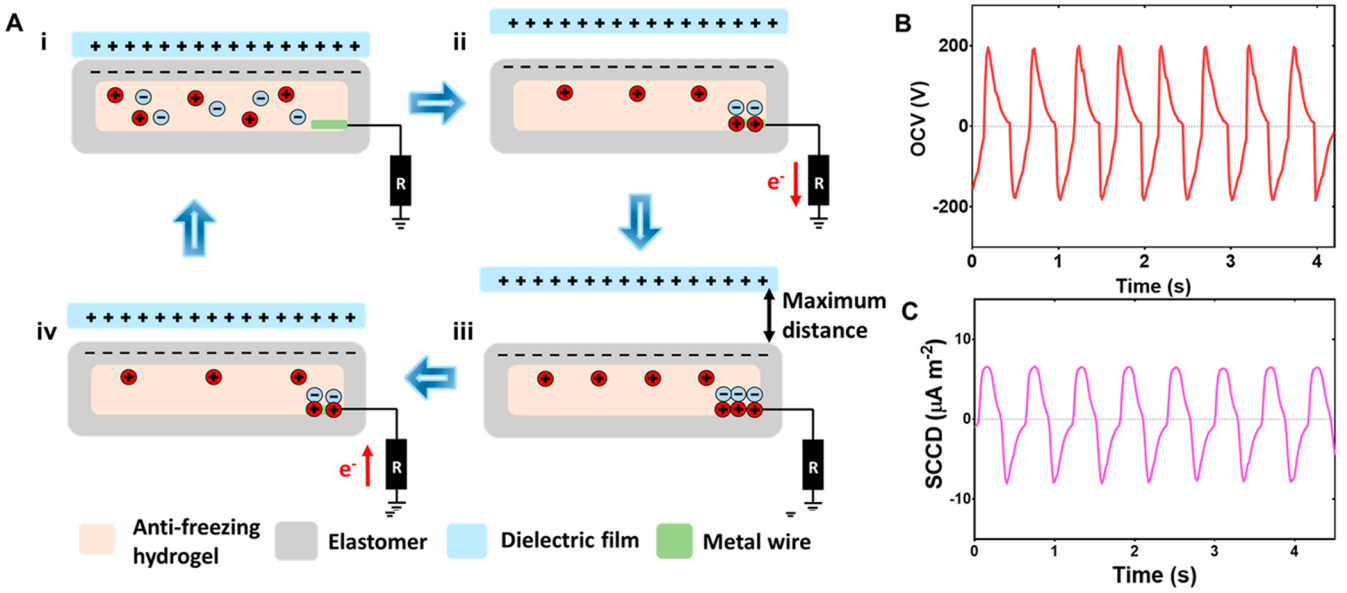

Figure 2. Working principle and output characteristics of the iTENG at single-electrode mode. (A) Schematic diagrams of the working principle of the iTENG. (B) Open-circuit voltage (OCV) and (C) short-circuit current density (SCCD) of an iTENG across a resistor (R = 3000 MΩ). The contact force was controlled at 6.03 N.

biological samples from icing damage at subzero temperatures because of their capability of hindering the ice crystallization of water molecules.[52] Here, glycerol was incorporated into the tough hydrogel matrix as a hygroscopic and cryoprotective chemical because it is nontoxic and thus suitable for wearable applications. In addition, the nonionic, kosmotropic characteristic of glycerol imposes minimal impact on the mechanical properties of tough hydrogel with ionic cross-links.[53] The inorganic ions used here are sodium (Na^+) and chloride (Cl^-) monoions since sodium chloride (NaCl) shows low biotoxicity at high concentrations and good electrical conductivity. It has been previously demonstrated that the presence of electrolyte salt contributes to the high ionic conductivity at room temperature (0.904 S m^{-1}), regardless the negative effect from glycerol.[34] The resistance of this conductive antifreezing hydrogel was observed to increase steadily with tensile strain,[34] but the increase rate was much slower than that of other traditionally stretchable electronic conductors[17] in the strain range of 0−300%. In addition, this resistance increase was much smaller than the inherent impedance of a TENG (at the order of MΩ) and thus had little negative impact on the TENG's output performance.[54]

One important design consideration of the iTENG is the interfacial bonding between the Alg−PAAm hydrogel (hydrophilic) and the two elastomer films (largely hydrophobic), which is naturally weak and has been proven to reduce the mechanical reliability and ambient stability of hydrogel-based TENGs.[49] In this work, the Alg−PAAm hydrogel was bonded to the Ecoflex by using a recently developed covalent bonding strategy, which revealed the highest hydrogel−elastomer adhesion energy ever reported.[55,56] With the treatment of the Ecoflex surface with 10 wt % benzophenone (an ultraviolet-assisted grafting agent) in ethanol solution, the PAAm prehydrogel polymers can chemically graft methacrylate groups on the Ecoflex surface during the PAAm covalent cross-linking (Figure 1C).[55] Before bonding the DN hydrogel layer and the two elastomer layers into an iTENG, we conducted a 2.5 h solvent exchange process to partially replace the water molecules in the DN hydrogel with glycerol and incorporate the electrolyte ions. The detailed fabrication procedure can be found in Figure S1 and the Materials and Methods section. As a result, the robust hydrogel−Ecoflex bonding interface can withstand at least 300% strain with no visible delamination occurring at the interface (Figure 1D). This strain level is higher than the maximum strain caused by normal human motions and most soft robot deformations.[34,57] In the meanwhile, we observed certain bubble-like fractures from the hydrogel-Ecoflex interface (Figure 1D). Our experiments show that it has little impact on the integration of iTENG and its performance. This fracture can also be addressed by directly bonding the hydrogel layer with two elastomers.[58]

Electrical Properties of the iTENG. Considering its application for wearable and stretchable electronics, we characterized the iTENG in the single-electrode mode by simply connecting the antifreezing ionic hydrogel to the ground by a metal wire through an external load (Figure 2A). A contact layer (e.g., skin, nylon, and stainless steel) and the Ecoflex coating layer of the iTENG serve as the positive and negative triboelectric layers,[59] respectively (Figure 2A). The energy harvesting of the iTENG is based on the coupling effect of contact electrification and electrostatic induction between the two triboelectric layers. Before a mechanical force is applied to the iTENG, there is no contact between the two triboelectric layers. Therefore, no surface charges are generated on two layers. As a result, the Na^+ and Cl^- ions inside the ionic hydrogel remain randomly distributed across the entire hydrogel matrix. Once the dielectric layer contacts the Ecoflex layer upon the application of a mechanical force, electrification occurs at the interface. Specifically, charges are transferred from the dielectric layer to the Ecoflex layer due to their different levels of electronegativity, leading to the same amount of positive and negative charges generated on the dielectric layer and the Ecoflex layer, respectively (Figure 2A-i).[18] While the two triboelectric layers still contact each other, there is no electric potential difference measured across these two layers.[35] When the dielectric film moves away from the elastomer, those

https://doi.org/10.1021/acsaelm.2c00118
ACS Appl. Electron. Mater. 2022, 4, 1930−1938

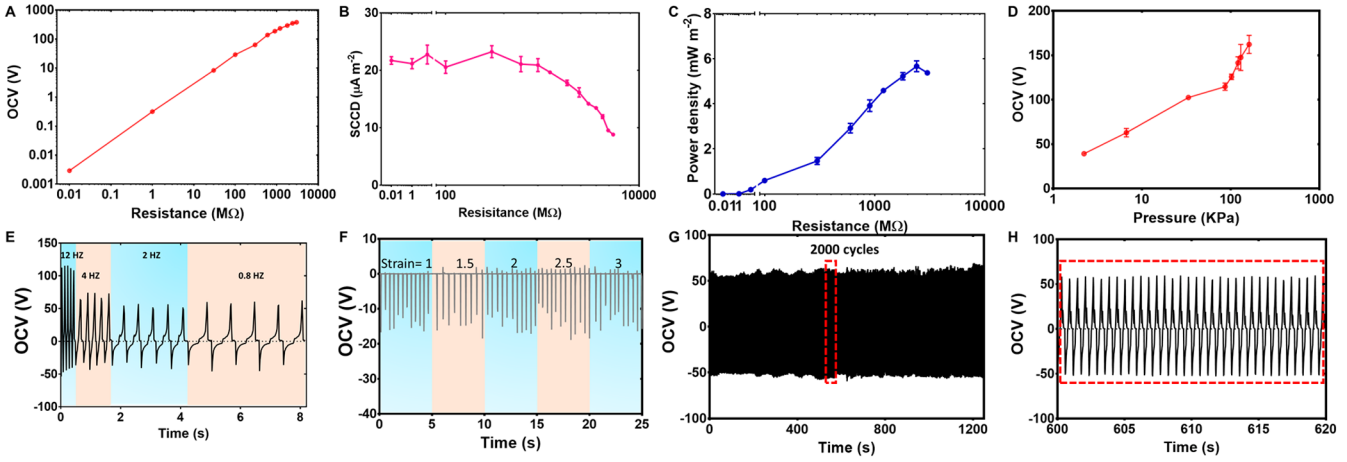

Figure 3. Electrical properties of the iTENG under different conditions. Variation of the output (A) voltage, (B) current density, and (C) power density with the external loading resistance. N = 5. Variation of peak amplitudes of the output voltage across the resistor (300 MΩ) for different contact (D) pressure and (E) frequency. (F) Variation of the output voltage across the resistor (600 MΩ) at different stretched length upon one finger tapping exerted at a force of 10 N and a frequency of 2 Hz. Output voltage stability of the iTENG when subjected to (G) 2000 cycles of contact separation motions and its (H) zoom-in view.

two oppositely charged surfaces separate and reveal an electric potential difference (measured as an open-circuit voltage, OCV). The unscreened negative charges on the elastomer surface will induce the movement of the positive ions (Na^+) in the ionic hydrogel to accumulate at the hydrogel−elastomer interface, balancing the static charges (Figure 2A-ii). In the meanwhile, negative ions (Cl^-) move and accumulate at the hydrogel−metal interface, leading to the formation of an electrical double layer; transient charges flow from the metal wires to the ground through the external load, generating a voltage output (Figure 2A-ii). This electrostatic induction reaches the equilibrium until the separation distance between the two charged surfaces reaches its maximum (Figure 2A-iii). Upon moving the dielectric film back to the elastomer, the whole process reverses, resulting in an electron flux with the opposite direction flow from the ground to the metal/hydrogel interface through the external load (Figure 2A-iv). By repeating the contact-separation movements between the dielectric object and the iTENG, cyclic alternating current and voltage can be generated.

The electrical performance of the iTENG was evaluated by measuring the OCV and the short-circuit current (SCC) generated by an iTENG. A pork skin or stainless-steel film was used to serve as the contact layer for repeated contact and separation with an iTENG (3 × 3 cm^2). Unless mentioned elsewhere, the contact frequency (∼2 Hz) of the contact-separation movement and the contact force (6.03 N) between the two contacting films are controlled to be the same by a linear motor for all following tests. Figures 2B and 2C show the representative OCV and SCC density (SCCD) curves measured by using a stainless-steel contact layer. With an external load resistance of 3000 MΩ, the iTENG generated a peak−peak OCV of 380 V (Figure 2B) and a peak−peak SCCD of 14.5 A m^{-2} (Figure 2C). As the impedance of the external load affects the energy-harvesting performance of TENGs, the OCV and SCCD of the iTENG were evaluated across various load resistances. Figures 3A and 3B show the testing data of the OCV and SCCD as a function of the load resistance. The OCV increased with the load resistance due to the voltage divider mechanism. The SCCD stayed in its plateau before 300 MΩ and then decreased gradually with the load resistance, which can be explained by the fact that the initial resistance increase was much smaller than the inherent impedance of iTENG.[54] Figure 3C shows that the output power density (calculated by the product of the OCV and SCCD) reaches a maximum of 5.7 mW m^{-2} at an external load resistance of 2400 MΩ. Antifreezing hydrogels with higher conductivity and elastomer films with micro/nano structures can be designed to further enhance the output power density of the iTENG.[35]

As the iTENG can be potentially used for self-powered mechanical sensing, we then characterized the electrical response of the iTENG under different applied pressures. Figure 3D shows that the peak−peak OCV value across a load resistor of 300 MΩ increases with the applied pressure magnitude (contact frequency: 2 Hz). A higher pressure can increase the effective contact area between the contact layer and the iTENG, thus enhancing the OCV output.[46] In addition, the iTENG can be utilized as a sustainable wearable energy harvester based on body motions with different frequencies (e.g., breath, heartbeat, walking and running). We evaluated the OCV output of the iTENG as a function of the contact frequency in the range of common body motions (≤12 Hz). As shown in Figure 3E, the peak amplitude of OCV increases with the contact frequency in the range 0.8−12 Hz and reaches a maximum value of 150 V under an applied force of 40.5 N across a load resistor of 300 MΩ. We also studied the electrical performance of iTENG upon large strain. We controlled the contact area to be approximately constant through tapping by an artificial finger structure with an exerted force of 10 N and a frequency of 2 Hz. Under this condition, the iTENG was able to maintain a stable performance with a peak voltage of around 15 V (across a load resistor of 600 MΩ) in the strain range of <200% (already larger than the maximum strain level caused by human motion) (Figure 3F). The OCV output repeatability of the iTENG was tested over 2000 cycles of contact-separation movement (pork skin was used as the contact layer to mimic human skin in wearable applications). The device showed a stable OCV output across an external load resistor of 300 MΩ under an applied force of 7.83 N (Figure 3G,H), indicating the suitability of the iTENG as a wearable device for long-term use.

https://doi.org/10.1021/acsaelm.2c00118
ACS Appl. Electron. Mater. 2022, 4, 1930−1938

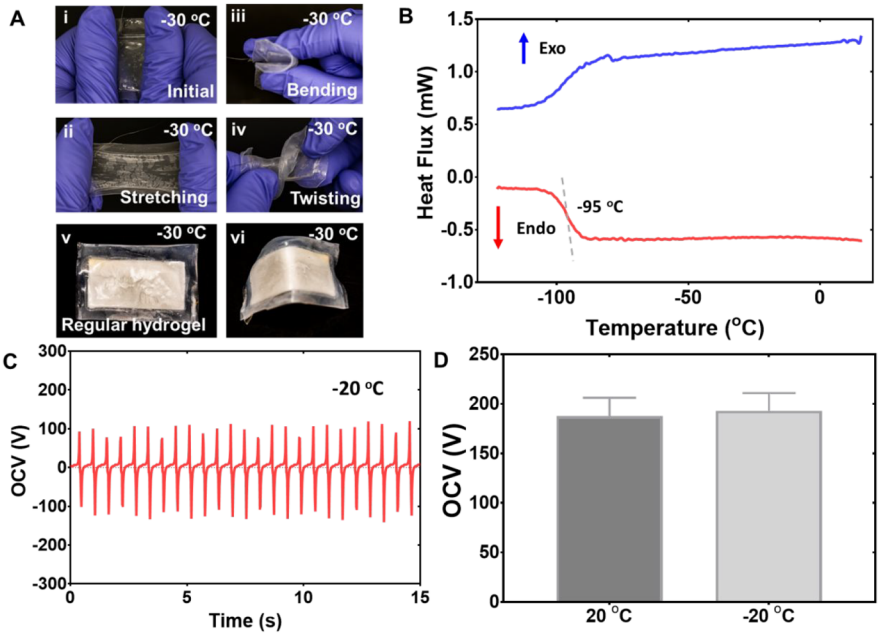

Figure 4. Antifreezing properties of the iTENG. (A) Photographs of an iTENG without freezing which can be twisted, bent, and stretched at −30 °C. (B) Dynamic scanning calorimetry (DSC) testing of the conductive hydrogel of an antifreezing iTENG in the temperature range of −120 to 15 °C. (C) Open-circuit voltage of an iTENG operating at −20 °C. (D) Comparison of the peak−peak OCV values at 20 °C and −20 °C (N = 4).

Antifreezing Properties of the iTENG. One concern about the practical use of hydrogel-based devices is the freezing of the aqueous content in the hydrogel at subzero temperatures, which makes the hydrogel mechanically rigid and electrically nonconductive.[34] Considering the great promise of the iTENG as a sensing and energy harvesting unit for wearable electronics, we then examined the antifreezing properties of the iTENG in freezing environments. Here, glycerol (66.6 wt %) dissolved in saturated NaCl solution (5.4 M) was used to soak the tough hydrogel to optimize its amount of unfrozen bound water and enhance its antifreezing property.[60] Indeed, the treated iTENG showed excellent freezing tolerance with good mechanical flexibility and stretchability (Figure 4A) after storage at −30 °C for 24 h because of the large amount of unfrozen bound water. We further determined the antifreezing limits of the iTENG through differential scanning calorimetry (DSC) from −120 to 15 °C. Notably, the antifreezing hydrogel did not show any cold-crystallization peak in the entire exo/cooling thermogram or any melting peak in the whole endo/heating thermogram (Figure 4B); this observation confirms that the antifreezing hydrogel did not frozen in the temperature range of −120 to 15 °C, which is consistent with the results of a previous report.[52] During heating, the antifreezing hydrogel only showed a peak similar to a glass transition at −95 °C (Figure 4B), indicating no observable icing of the hydrogels. This antifreezing performance is better than most of the previously reported ionic hydrogels.[34] In addition, the Ecoflex has been known to have an extremely low freezing limit of −53.8 °C.[61] Moreover, our previous work has reported that the antifreezing hydrogel showed high conductivity under extremely cold environment (5.34×10^{-2} S m^{-1} at −25 °C, 8.7×10^{-3} S m^{-1} at −40 °C, and 1.96×10^{-5} S m^{-1} at −70 °C).[34] The good conductivity and mechanical deformability of both the hydrogel and the Ecoflex at low temperatures are essential to realize stretchable self-powering sensors and energy harvesters capable of operating in extremely cold environments. To further verify the self-powering efficiency of the iTENG at low temperatures, we also evaluated its electrical output performance at −20 °C (Figure 4C), and this characterization temperature can be further down to a lower level (e.g., −50 °C) by involving a linear motor that can work properly in such a harsh condition. The OCV output of the iTENG at −20 °C was similar to that at 20 °C (Figure 4D), with the same testing conditions (i.e., external load resistance: 300 MΩ; applied force: 350 N; contact-separation frequency: 2 Hz). These results indicate that the iTENG has good antifreezing properties and could serve as a stretchable and self-powering sensor or energy harvester for use in extremely cold environments.

Demonstration of Mechanical Energy Harvesting. The superior energy-harvesting performance along with extremely stretchable and antifreezing features makes the iTENG an ideal sustainable power source for the realization of self-powered electronics. The iTENG could be used to directly drive external electronics for real-time applications by scavenging biomechanical energy, especially the energy of human motions. A pack of 30 blue light-emitting diodes (LEDs) connected in series were driven by the iTENG to send a warning signal of "S", "O", "S" upon tapping of the iTENG (Figure 5A,B and Movie S1). The iTENG was tapped by a human hand at ∼2 Hz.

Furthermore, the energy-harvesting ability of the iTENG under extremely cold environments was demonstrated by charging a capacitor that was then used to power electronics, as shown in Figure 5C. The detailed circuit diagram is illustrated in Figure 5D. For demonstration, an iTENG was first stored in a fridge (−20 °C) for at least 3 h to reach equilibrium and then tapped by the hand at −20 °C to charge a capacitor of 10 μF (through a bridge rectifier) and to power a digital clock thereafter (Figure 5C and Movie S2). The tapping frequency is about 2 Hz, and the representative current after rectification is

https://doi.org/10.1021/acsaelm.2c00118
ACS Appl. Electron. Mater. 2022, 4, 1930−1938

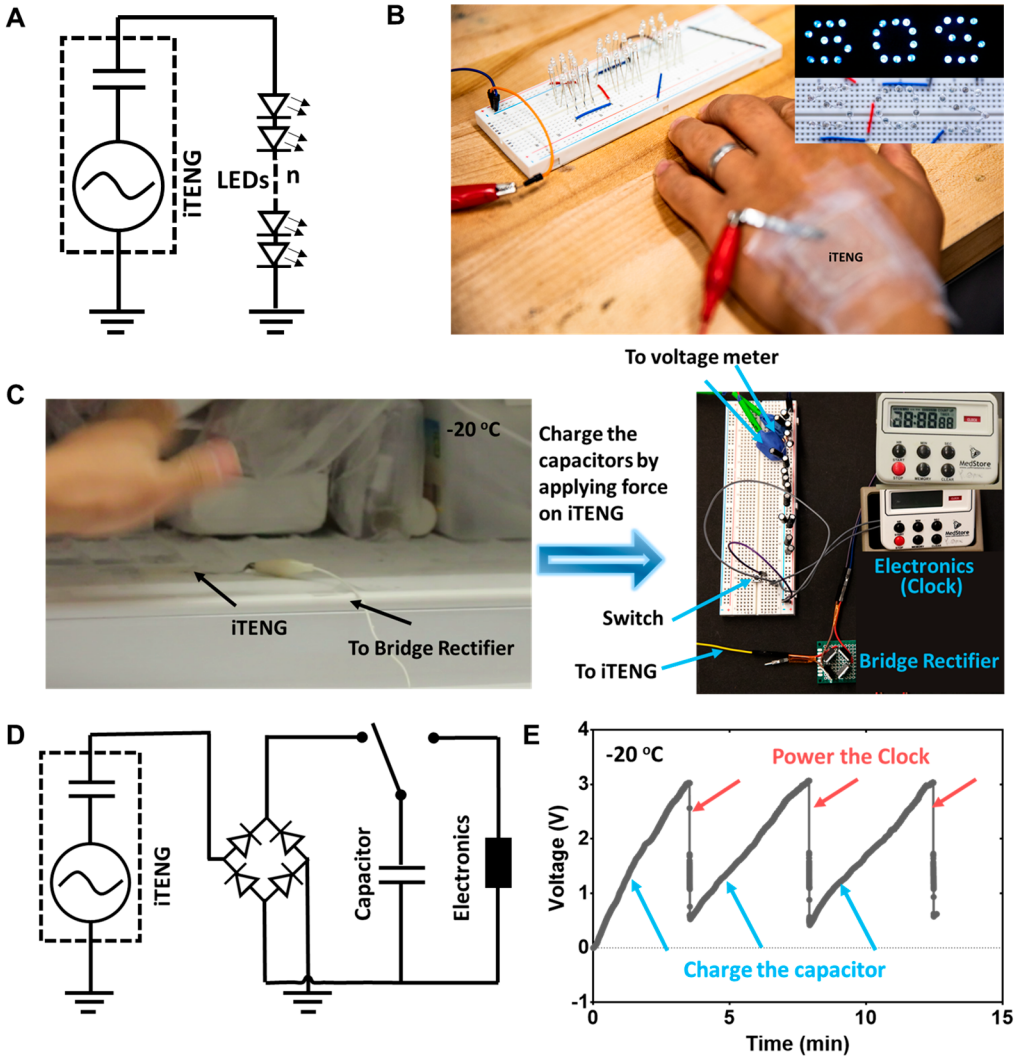

Figure 5. Biomechanical energy harvesting by the iTENG at room and subzero temperatures. (A) The equivalent circuit to light the multiple LEDs connected in series by tapping the iTENG at single-electrode mode. (B) An image of 30 blue LEDs lightened by tapping the iTENG to send the warn signal of "S", "O", "S", operating at room temperature. (C) Images of an antifreezing iTENG in the fridge (−20 °C) and its rectifier and charging circuits to power an electronic clock. (D) The equivalent circuit diagram of the self-charging system that uses the energy harvested from the iTENG to power the electronic clock. (E) Voltage profile of a 10 μF capacitor being charged by tapping the iTENG and then used to power the electronic clock at −20 °C.

shown in Figure S3. In ∼204 s, the voltage of the capacitor could be increased linearly to 3 V, which can then power the clock (Figure 5C,E and Movie S2). Subsequently, the capacitor can be charged back to 3 V in ∼240 s, powering the clock repeatedly (Figure 5E). These demonstrations confirm that our iTENG could act as stretchable and wearable self-powered electronics as well as sustainable power sources in both regular and extremely cold conditions.

■ CONCLUSION

In summary, we reported a novel antifreezing ionic triboelectric nanogenerator (iTENG), made from a dielectric elastomer and freeze-tolerant ionic hydrogel as the electrification layer and the electrode, respectively. The simple structural design of the iTENG realized a high stretchability of more than 300%, fully satisfying the mechanical requirement of skin-like wearable sensors. By incorporating glycol and NaCl, the iTENG also maintained its stable electrical energy-harvesting characteristics under both the regular condition and extremely cold temperatures (down to −53 °C). The iTENG converted mechanical stimuli into OCV and SCCD outputs, which can be used for energy harvesting and self-powered sensing. The iTENG was calibrated in OCV and SCCD modes under different levels of the external loading resistance, contact pressure and frequency, stretch, and environment temperature. In addition, for the robust interfacial bonding between hydrogel and elastomer, the iTENG showed a good mechanical durability (2000 times) under cyclic compression without electrical degradation. For proof of demonstration, the iTENG was demonstrated as a sustainable and effective biomechanical energy harvester, which can drive an electronic device by using biomechanical stimuli from various human motions in both regular and extremely cold environments. We envision that the iTENG will have great potential for the next-generation wearable electronics and soft robotics.

https://doi.org/10.1021/acsaelm.2c00118
ACS Appl. Electron. Mater. 2022, 4, 1930−1938

MATERIALS AND METHODS

Materials. The ionic cross-linker calcium sulfate ($CaSO_2$, 255548), Alginate (A2033), acrylamide (AAm, A8887), covalent cross-linker *N*,*N*′-methylenebis(acrylamide) (MBAA, M7279), photoinitiator IRGACURE 2959 (I2959), acetic acid (695092), sodium chrolide, bridging polymer chitosan of medium molecular weight (448877), the coupling reagents, 1-ethyl-3-(3-(dimethylamino)-propyl)carbodiimide hydrochloride (EDC, E1769), hydroxysulfosuccinimide (sulfo-NHS, 56485), and hygroscopic substance glycerol (G9012) were purchased from Sigma. Milli-Q (18.3 MΩ) water was used in all experiments. Porcine skin was purchased from a local grocery store.

Fabrication of the iTENG. The fabrication of the iTENG consists of three steps (Figure S1): (i) the fabrication of tough alginate−polyacrylamide (Alg-PAAm) DN hydrogel−elastomer bilayered structure, (ii) solvent exchange, and (iii) the bonding of two hydrogel−elastomer bilayers and the device assembly.

The hydrogel−elastomer bilayer structure was prepared based on the modified method reported previously.[19] In brief, the precured Ecoflex A and B (00-30, Smooth-On Inc.) were mixed quickly and spin-coated on a hydrophobic glass slide. After curing on the hot plate (80 °C) for 40 min, the surfaces of Ecoflex were thoroughly cleaned with methanol and deionized water and completely dried with nitrogen gas before the benzophenone treatment. After that, benzophenone solution (10 wt % in ethanol) was applied onto the elastomer to evenly cover the entire elastomer surface for 15 min at room temperature. Then, the elastomer was washed with methanol three times and completely dried with nitrogen gas before use. Hydrogel was prepared by mixing 10 mL of a carefully degassed aqueous pregel solution (12 wt % AAm, 2 wt % sodium alginate, and 36 μL of 2 wt % MBAA) with ionic cross-linkers (191 μL of 0.75 M $CaSO_4$ slurries) and Irgacure 2959 (0.2 wt %). The mixture was then stirred quickly, poured onto the freshly treated elastomer film, and then covered by glass plate with hydrophobic coating. The whole assembled mold was followed by ultraviolet irradiation in a 254 nm ultraviolet chamber (28−32 mW cm^{-2}, UVO-Cleaner 42A, Jelight Company, Inc.) for an hour, during which the PAAm network was covalently cross-linked and bonded onto elastomer surface.

Next, hygroscopic reagents and electrolyte salt were soaked into the ionic hydrogel layer to increase its ambient stability, antifreezing capability, and ionic conductivity. Generally, the ionic hydrogel can reach the equilibrium state once immersed in the conductive hygroscopic solvent for 2.5 h exchanging as reported previously.[52] Unless noted elsewhere, the conductive hygroscopic solvent for exchanging was prepared by adding glycerol to the saturated NaCl aqueous solution (5.4 M), and the weight ratio of glycerol to distilled water is 2:1 due to the fact that 66.6 wt % of glycerol in a glycerol−water mixture can achieve the lowest freezing temperature.[60] To ensure the concentrations of NaCl and glycerol in the external solution remained nearly constant before and after soaking the hydrogel, we prepared the solvent solution with a volume 20 times that of the hydrogel.

Before bonding, all visible liquid was carefully removed from the hydrogel surface. The bridging polymer chitosan was dissolved into distilled water at 2.0 wt %, and the pH was adjusted to 5.5−6 by acetic acid. EDC and NHS were used as the coupling reagents. The final concentrations of EDC and NHS in the solution of the bridging polymer were both 12 mg/mL. The mixture of the bridging polymer and coupling reagents was applied on one hydrogel surface and then gently pressed on another hydrogel surface for at least 1 h for carbodiimide coupling reaction. Finally, the surrounding Ecoflex edge was sealed by the degassed precured Ecoflex.

Characterization and Measurements. A linear motor was used to provide the input of mechanical motions (Figure S2). For all the tests of energy generation of the iTENG, the voltage and current were recorded by a Keithley 2614B source meter. The force applied by the motor was detected by a force sensor. For the measurement of the output performances of the iTENG at subzero temperatures, the iTENG along with the linear motor was kept inside a fridge (−20 °C).

Antifreezing Characterization. The freezing point of samples was characterized by using a differential scanning calorimeter (TA Instruments, DSC 2920) with a mechanical cooling system. Samples (5−10 mg) were contained in hermetically sealed aluminum pans (TA Instruments, Tzero Aluminum Hermetic Pan) for testing, with an empty pan used as the reference. The DSC was operated under a 35 μL min^{-1} nitrogen flow rate, and data were captured at a rate of 5 Hz. Samples were cooled at a rate of 2 °C min^{-1} to −120 °C. After an isothermal period of 30 min, samples were heated at 2 °C min^{-1} to the initial equilibration temperature (15 °C).

Statistical Analysis. Statistical analyses were performed on GraphPad Prism software (GraphPad Software, Inc.). Results are depicted as mean ± standard deviation (SD); we conducted unpaired Student's *t*-test to analyze the statistical differences of experiment results. We used the parametric test and assumed any experimental groups are normally distributed with the same SD. Differences were considered statistically significant if $P < 0.05$.

Testing of the iTENG on Human Hand. The tests of the devices on human body described here do not need Institutional Review Board (IRB) approval because our experiments do not affect living people physically or physiologically, and we have not sought or received identifiable private information. The hand shown in Figures 1, 4 and 5 as well as in Movies S1 and S2 are those of B. Ying, who has given his consent to publish these images.

ASSOCIATED CONTENT

Supporting Information

The Supporting Information is available free of charge at https://pubs.acs.org/doi/10.1021/acsaelm.2c00118.

Fabrication, characterization setup, and rectified current output of the iTENG (PDF)

Movie S1: An iTENG was tapping by hand to drive 30 blue light-emitting diodes (LEDs) connected in series to send the warn signal of "SOS" (MP4)

Movie S2: An iTENG stored at −20 °C was tapping by hand to charge a 10 μF capacitor to power an digital clock for multiple times (MP4)

AUTHOR INFORMATION

Corresponding Author

Xinyu Liu − *Department of Mechanical and Industrial Engineering, University of Toronto, Toronto, ON M5S 3G8, Canada; Institute of Biomedical Engineering, University of Toronto, Toronto, ON M5S 3G9, Canada;* orcid.org/0000-0001-5705-9765; Email: xyliu@mie.utoronto.ca

Authors

Binbin Ying − *Department of Mechanical and Industrial Engineering, University of Toronto, Toronto, ON M5S 3G8, Canada; Department of Mechanical Engineering, McGill University, Montreal, QC H3A 0C3, Canada;* Present Address: Department of Mechanical Engineering, Massachusetts Institute of Technology, 77 Massachusetts Avenue, Cambridge, MA 02139

Runze Zuo − *Department of Mechanical and Industrial Engineering, University of Toronto, Toronto, ON M5S 3G8, Canada*

Yilun Wan − *Department of Mechanical and Industrial Engineering, University of Toronto, Toronto, ON M5S 3G8, Canada*

Complete contact information is available at: https://pubs.acs.org/10.1021/acsaelm.2c00118

https://doi.org/10.1021/acsaelm.2c00118
ACS Appl. Electron. Mater. 2022, 4, 1930−1938

Notes

The authors declare no competing financial interest.

■ ACKNOWLEDGMENTS

This work was supported by the Natural Sciences and Engineering Research Council of Canada (RGPIN2017-06374 and RGPAS 507980-17), the Canada Foundation for Innovation (JELF-38428), and the University of Toronto. B.Y. thanks the NSERC Postdoctoral Fellowships Program (PDF-557493-2021).

■ REFERENCES

(1) Hu, L.; Choi, J. W.; Yang, Y.; Jeong, S.; La Mantia, F.; Cui, L.-F.; Cui, Y. Highly Conductive Paper for Energy-Storage Devices. *Proc. Natl. Acad. Sci. U. S. A.* **2009**, *106* (51), 21490−21494.
(2) Pushparaj, V. L.; Shaijumon, M. M.; Kumar, A.; Murugesan, S.; Ci, L.; Vajtai, R.; Linhardt, R. J.; Nalamasu, O.; Ajayan, P. M. Flexible Energy Storage Devices Based on Nanocomposite Paper. *Proc. Natl. Acad. Sci. U. S. A.* **2007**, *104* (34), 13574−13577.
(3) Scrosati, B. Paper Powers Battery Breakthrough. *Nat. Nanotechnol.* **2007**, *2* (10), 598−599.
(4) Hu, L.; Wu, H.; La Mantia, F.; Yang, Y.; Cui, Y. Thin, Flexible Secondary Li-Ion Paper Batteries. *ACS Nano* **2010**, *4* (10), 5843−5848.
(5) Yoon, J.; Jo, S.; Chun, I. S.; Jung, I.; Kim, H.-S.; Meitl, M.; Menard, E.; Li, X.; Coleman, J. J.; Paik, U.; Rogers, J. A. GaAs Photovoltaics and Optoelectronics Using Releasable Multilayer Epitaxial Assemblies. *Nature* **2010**, *465* (7296), 329−333.
(6) Peet, J.; Kim, J. Y.; Coates, N. E.; Ma, W. L.; Moses, D.; Heeger, A. J.; Bazan, G. C. Efficiency Enhancement in Low-Bandgap Polymer Solar Cells by Processing with Alkane Dithiols. *Nat. Mater.* **2007**, *6* (7), 497−500.
(7) Xu, S.; Qin, Y.; Xu, C.; Wei, Y.; Yang, R.; Wang, Z. L. Self-Powered Nanowire Devices. *Nat. Nanotechnol.* **2010**, *5* (5), 366−373.
(8) Wang, S.; Lin, L.; Wang, Z. L. Nanoscale Triboelectric-Effect-Enabled Energy Conversion for Sustainably Powering Portable Electronics. *Nano Lett.* **2012**, *12* (12), 6339−6346.
(9) Bae, J.; Lee, J.; Kim, S.; Ha, J.; Lee, B.-S.; Park, Y.; Choong, C.; Kim, J.-B.; Wang, Z. L.; Kim, H.-Y.; Park, J.-J.; Chung, U-I. Flutter-Driven Triboelectrification for Harvesting Wind Energy. *Nat. Commun.* **2014**, *5* (1), 1−9.
(10) Chun, J.; Ye, B. U.; Lee, J. W.; Choi, D.; Kang, C.-Y.; Kim, S.-W.; Wang, Z. L.; Baik, J. M. Boosted Output Performance of Triboelectric Nanogenerator Via Electric Double Layer Effect. *Nat. Commun.* **2016**, *7* (1), 1−9.
(11) Wang, S.; Lin, L.; Wang, Z. L. Triboelectric Nanogenerators as Self-Powered Active Sensors. *Nano Energy* **2015**, *11*, 436−462.
(12) Wang, Z. L.; Chen, J.; Lin, L. Progress in Triboelectric Nanogenerators as a New Energy Technology and Self-Powered Sensors. *Energy Environ. Sci.* **2015**, *8* (8), 2250−2282.
(13) Chen, G.; Fang, Y.; Zhao, X.; Tat, T.; Chen, J. Textiles for Learning Tactile Interactions. *Nature Electronics* **2021**, *4* (3), 175−176.
(14) Chen, G.; Li, Y.; Bick, M.; Chen, J. Smart Textiles for Electricity Generation. *Chem. Rev.* **2020**, *120* (8), 3668−3720.
(15) Chen, X.; Pu, X.; Jiang, T.; Yu, A.; Xu, L.; Wang, Z. L. Tunable Optical Modulator by Coupling a Triboelectric Nanogenerator and a Dielectric Elastomer. *Adv. Funct. Mater.* **2017**, *27* (1), 1603788.
(16) Yi, F.; Lin, L.; Niu, S.; Yang, P. K.; Wang, Z.; Chen, J.; Zhou, Y.; Zi, Y.; Wang, J.; Liao, Q.; Zhang, Y.; Wang, Z. L. Stretchable-Rubber-Based Triboelectric Nanogenerator and Its Application as Self-Powered Body Motion Sensors. *Adv. Funct. Mater.* **2015**, *25* (24), 3688−3696.
(17) Hwang, B.-U.; Lee, J.-H.; Trung, T. Q.; Roh, E.; Kim, D.-I.; Kim, S.-W.; Lee, N.-E. Transparent Stretchable Self-Powered Patchable Sensor Platform with Ultrasensitive Recognition of Human Activities. *ACS Nano* **2015**, *9* (9), 8801−8810.
(18) Lai, Y. C.; Deng, J.; Niu, S.; Peng, W.; Wu, C.; Liu, R.; Wen, Z.; Wang, Z. L. Electric Eel-Skin-Inspired Mechanically Durable and Super-Stretchable Nanogenerator for Deformable Power Source and Fully Autonomous Conformable Electronic-Skin Applications. *Adv. Mater.* **2016**, *28* (45), 10024−10032.
(19) Yi, F.; Wang, X.; Niu, S.; Li, S.; Yin, Y.; Dai, K.; Zhang, G.; Lin, L.; Wen, Z.; Guo, H.; et al. A Highly Shape-Adaptive, Stretchable Design Based on Conductive Liquid for Energy Harvesting and Self-Powered Biomechanical Monitoring. *Sci. Adv.* **2016**, *2* (6), No. e1501624.
(20) Zhang, P.; Chen, Y.; Guo, Z. H.; Guo, W.; Pu, X.; Wang, Z. L. Stretchable, Transparent, and Thermally Stable Triboelectric Nanogenerators Based on Solvent-Free Ion-Conducting Elastomer Electrodes. *Adv. Funct. Mater.* **2020**, *30* (15), 1909252.
(21) Liu, Z.; Wang, Y.; Ren, Y.; Jin, G.; Zhang, C.; Chen, W.; Yan, F. Poly (Ionic Liquid) Hydrogel-Based Anti-Freezing Ionic Skin for a Soft Robotic Gripper. *Materials Horizons* **2020**, *7* (3), 919−927.
(22) Sun, L.; Chen, S.; Guo, Y.; Song, J.; Zhang, L.; Xiao, L.; Guan, Q.; You, Z. Ionogel-Based, Highly Stretchable, Transparent, Durable Triboelectric Nanogenerators for Energy Harvesting and Motion Sensing over a Wide Temperature Range. *Nano Energy* **2019**, *63*, 103847.
(23) Ren, Y.; Guo, J.; Liu, Z.; Sun, Z.; Wu, Y.; Liu, L.; Yan, F. Ionic Liquid-Based Click-Ionogels. *Sci. Adv.* **2019**, *5* (8), No. eaax0648.
(24) Yiming, B.; Han, Y.; Han, Z.; Zhang, X.; Li, Y.; Lian, W.; Zhang, M.; Yin, J.; Sun, T.; Wu, Z.; et al. A Mechanically Robust and Versatile Liquid-Free Ionic Conductive Elastomer. *Adv. Mater.* **2021**, *33* (11), 2006111.
(25) Ying, B.; Liu, X. Skin-Like Hydrogel Devices for Wearable Sensing, Soft Robotics and Beyond. *Iscience* **2021**, *24* (11), 103174.
(26) Yang, C.; Suo, Z. Hydrogel Ionotronics. *Nature Reviews Materials* **2018**, *3* (6), 125.
(27) Lee, H. R.; Kim, C. C.; Sun, J. Y. Stretchable Ionics-a Promising Candidate for Upcoming Wearable Devices. *Adv. Mater.* **2018**, *30* (42), 1704403.
(28) Sheng, H.; Wang, X.; Kong, N.; Xi, W.; Yang, H.; Wu, X.; Wu, K.; Li, C.; Hu, J.; Tang, J.; et al. Neural Interfaces by Hydrogels. *Extreme Mechanics Letters* **2019**, *30*, 100510.
(29) Bao, G.; Jiang, T.; Ravanbakhsh, H.; Reyes, A.; Ma, Z.; Strong, M.; Wang, H.; Kinsella, J. M.; Li, J.; Mongeau, L. Triggered Micropore-Forming Bioprinting of Porous Viscoelastic Hydrogels. *Materials horizons* **2020**, *7* (9), 2336−2347.
(30) Bao, G.; Huo, R.; Ma, Z.; Strong, M.; Valiei, A.; Jiang, S.; Liu, S.; Mongeau, L.; Li, J. Ionotronic Tough Adhesives with Intrinsic Multifunctionality. *ACS Appl. Mater. Interfaces* **2021**, *13* (31), 37849−37861.
(31) Taheri, S.; Bao, G.; He, Z.; Mohammadi, S.; Ravanbakhsh, H.; Lessard, L.; Li, J.; Mongeau, L. Injectable, Pore-Forming, Perfusable Double-Network Hydrogels Resilient to Extreme Biomechanical Stimulations. *Advanced Science* **2022**, *9* (2), 2102627.
(32) Ma, Z.; Yang, Z.; Gao, Q.; Bao, G.; Valiei, A.; Yang, F.; Huo, R.; Wang, C.; Song, G.; Ma, D.; Gao, Z.-H.; Li, J. Bioinspired Tough Gel Sheath for Robust and Versatile Surface Functionalization. *Sci. Adv.* **2021**, *7* (15), No. eabc3012.
(33) Alizadeh-Meghrazi, M.; Ying, B.; Schlums, A.; Lam, E.; Eskandarian, L.; Abbas, F.; Sidhu, G.; Mahnam, A.; Moineau, B.; Popovic, M. R. Evaluation of Dry Textile Electrodes for Long-Term Electrocardiographic Monitoring. *Biomedical engineering online* **2021**, *20* (1), 1−20.
(34) Ying, B.; Chen, R. Z.; Zuo, R.; Li, J.; Liu, X. An Anti-Freezing, Ambient-Stable and Highly Stretchable Ionic Skin with Strong Surface Adhesion for Wearable Sensing and Soft Robotics. *Adv. Funct. Mater.* **2021**, *31* (42), 2104665.
(35) Pu, X.; Liu, M.; Chen, X.; Sun, J.; Du, C.; Zhang, Y.; Zhai, J.; Hu, W.; Wang, Z. L. Ultrastretchable, Transparent Triboelectric Nanogenerator as Electronic Skin for Biomechanical Energy Harvesting and Tactile Sensing. *Sci. Adv.* **2017**, *3* (5), No. e1700015.
(36) Zhu, M.; Wang, X.; Tang, H.; Wang, J.; Hao, Q.; Liu, L.; Li, Y.; Zhang, K.; Schmidt, O. G. Antifreezing Hydrogel with High Zinc

https://doi.org/10.1021/acsaelm.2c00118
ACS Appl. Electron. Mater. 2022, 4, 1930−1938

Reversibility for Flexible and Durable Aqueous Batteries by Cooperative Hydrated Cations. *Adv. Funct. Mater.* **2020**, *30* (6), 1907218.
(37) Liu, X.; Liu, J.; Lin, S.; Zhao, X. Hydrogel Machines. *Mater. Today* **2020**, *36*, 102−124.
(38) Sun, J. Y.; Keplinger, C.; Whitesides, G. M.; Suo, Z. Ionic Skin. *Adv. Mater.* **2014**, *26* (45), 7608−7614.
(39) Lei, Z.; Wu, P. A Supramolecular Biomimetic Skin Combining a Wide Spectrum of Mechanical Properties and Multiple Sensory Capabilities. *Nat. Commun.* **2018**, *9* (1), 1134.
(40) Gu, G.; Xu, H.; Peng, S.; Li, L.; Chen, S.; Lu, T.; Guo, X. Integrated Soft Ionotronic Skin with Stretchable and Transparent Hydrogel-Elastomer Ionic Sensors for Hand-Motion Monitoring. *Soft robotics* **2019**, *6* (3), 368−376.
(41) Gu, G.; Zhang, N.; Xu, H.; Lin, S.; Yu, Y.; Chai, G.; Ge, L.; Yang, H.; Shao, Q.; Sheng, X.; Zhu, X.; Zhao, X. A Soft Neuroprosthetic Hand Providing Simultaneous Myoelectric Control and Tactile Feedback. *Nat. Biomed. Eng.* **2021**, 1−10.
(42) Shen, Z.; Zhu, X.; Majidi, C.; Gu, G. Cutaneous Ionogel Mechanoreceptors for Soft Machines, Physiological Sensing, and Amputee Prostheses. *Adv. Mater.* **2021**, *33* (38), 2102069.
(43) Ying, B.; Wu, Q.; Li, J.; Liu, X. An Ambient-Stable and Stretchable Ionic Skin with Multimodal Sensation. *Materials Horizons* **2020**, *7* (2), 477−488.
(44) Kim, C.-C.; Lee, H.-H.; Oh, K. H.; Sun, J.-Y. Highly Stretchable, Transparent Ionic Touch Panel. *Science* **2016**, *353* (6300), 682−687.
(45) Larson, C.; Peele, B.; Li, S.; Robinson, S.; Totaro, M.; Beccai, L.; Mazzolai, B.; Shepherd, R. Highly Stretchable Electroluminescent Skin for Optical Signaling and Tactile Sensing. *science* **2016**, *351* (6277), 1071−1074.
(46) Parida, K.; Kumar, V.; Jiangxin, W.; Bhavanasi, V.; Bendi, R.; Lee, P. S. Highly Transparent, Stretchable, and Self-Healing Ionic-Skin Triboelectric Nanogenerators for Energy Harvesting and Touch Applications. *Adv. Mater.* **2017**, *29* (37), 1702181.
(47) Yang, D.; Ni, Y.; Kong, X.; Li, S.; Chen, X.; Zhang, L.; Wang, Z. L. Self-Healing and Elastic Triboelectric Nanogenerators for Muscle Motion Monitoring and Photothermal Treatment. *ACS Nano* **2021**, *15* (9), 14653−14661.
(48) Lee, Y.; Cha, S. H.; Kim, Y.-W.; Choi, D.; Sun, J.-Y. Transparent and Attachable Ionic Communicators Based on Self-Cleanable Triboelectric Nanogenerators. *Nat. Commun.* **2018**, *9* (1), 1−8.
(49) Liu, T.; Liu, M.; Dou, S.; Sun, J.; Cong, Z.; Jiang, C.; Du, C.; Pu, X.; Hu, W.; Wang, Z. L. Triboelectric-Nanogenerator-Based Soft Energy-Harvesting Skin Enabled by Toughly Bonded Elastomer/Hydrogel Hybrids. *ACS Nano* **2018**, *12* (3), 2818−2826.
(50) Sun, J.-Y.; Zhao, X.; Illeperuma, W. R.; Chaudhuri, O.; Oh, K. H.; Mooney, D. J.; Vlassak, J. J.; Suo, Z. Highly Stretchable and Tough Hydrogels. *Nature* **2012**, *489* (7414), 133−136.
(51) Li, J.; Celiz, A. D.; Yang, J.; Yang, Q.; Wamala, I.; Whyte, W.; Seo, B. R.; Vasilyev, N. V.; Vlassak, J. J.; Suo, Z.; Mooney, D. J. Tough Adhesives for Diverse Wet Surfaces. *Science* **2017**, *357* (6349), 378−381.
(52) Chen, F.; Zhou, D.; Wang, J.; Li, T.; Zhou, X.; Gan, T.; Handschuh-Wang, S.; Zhou, X. Rational Fabrication of Anti-Freezing, Non-Drying Tough Organohydrogels by One-Pot Solvent Displacement. *Angew. Chem.* **2018**, *130* (22), 6678−6681.
(53) Williams, W. P.; Quinn, P. J.; Tsonev, L. I.; Koynova, R. D. The Effects of Glycerol on the Phase Behaviour of Hydrated Distearoylphosphatidylethanolamine and Its Possible Relation to the Mode of Action of Cryoprotectants. *Biochimica et Biophysica Acta (BBA)-Biomembranes* **1991**, *1062* (2), 123−132.
(54) Chen, X.; Miao, L.; Guo, H.; Chen, H.; Song, Y.; Su, Z.; Zhang, H. Waterproof and Stretchable Triboelectric Nanogenerator for Biomechanical Energy Harvesting and Self-Powered Sensing. *Appl. Phys. Lett.* **2018**, *112* (20), 203902.
(55) Yuk, H.; Zhang, T.; Parada, G. A.; Liu, X.; Zhao, X. Skin-Inspired Hydrogel-Elastomer Hybrids with Robust Interfaces and Functional Microstructures. *Nat. Commun.* **2016**, *7* (1), 1−11.
(56) Yang, J.; Bai, R.; Chen, B.; Suo, Z. Hydrogel Adhesion: A Supramolecular Synergy of Chemistry, Topology, and Mechanics. *Adv. Funct. Mater.* **2020**, *30* (2), 1901693.
(57) Ying, B.; Wu, Q.; Li, J.; Liu, X. An Ambient-Stable and Stretchable Ionic Skin with Multimodal Sensation. *Materials Horizons* **2020**, *7* (2), 477−488.
(58) Zuo, R.; Zhou, Z.; Ying, B.; Liu, X. A Soft Robotic Gripper with Anti-Freezing Ionic Hydrogel-Based Sensors for Learning-Based Object Recognition. In *2021 IEEE International Conference on Robotics and Automation (ICRA)*, 2021; IEEE: pp 12164−12169.
(59) Wang, Z. L. Triboelectric Nanogenerators as New Energy Technology for Self-Powered Systems and as Active Mechanical and Chemical Sensors. *ACS Nano* **2013**, *7* (11), 9533−9557.
(60) Lane, L. B. Freezing Points of Glycerol and Its Aqueous Solutions. *Ind. Eng. Chem.* **1925**, *17* (9), 924−924.
(61) Ecoflex 00-30. https://www.smooth-on.com/products/ecoflex-00-30/ (accessed 2020-08-29).

https://doi.org/10.1021/acsaelm.2c00118
ACS Appl. Electron. Mater. 2022, 4, 1930−1938